

# 3,8-Diaminobenzo[*c*]Cinnoline Derivatived Graphene Oxide Modified Graphene Oxide Sensor for the Voltammetric Determination of Cd<sup>2+</sup> and Pb<sup>2+</sup>

Gamze Kuzu Çelik<sup>1</sup> · Ahmet Ferat Üzdürmez<sup>2</sup> · Aslı Erkal<sup>1</sup> · Emine Kılıç<sup>2</sup> · Ali Osman Solak<sup>3</sup> · Zafer Üstündağ<sup>1</sup>

Published online: 23 January 2016  
© Springer Science+Business Media New York 2016

**Abstract** Highly sensitive 3,8-diaminobenzo[*c*]cinnoline (3,8-DABCC) modified graphene oxide (GO) electrode was prepared, and it was denoted as pGO-DABCC. The electrode material was characterized with infrared spectroscopy (IR), X-ray photoelectron spectroscopy (XPS), cyclic voltammetry (CV), and electrochemical impedance spectroscopy (EIS). pGO-DABCC on glassy carbon (GC/pGO-DABCC) electrode was investigated for simultaneous determination of Cd<sup>2+</sup> and Pb<sup>2+</sup> in aqueous media by differential pulse anodic stripping voltammetry (DPASV). Optimum conditions of the electrode were determined with some parameters such as constant potential, incubation time, pH, and volume of suspension on the electrode. The calibration equations for Cd<sup>2+</sup> and Pb<sup>2+</sup> determination were calculated as  $I_p(\mu\text{A}) = 0.3606[\text{Cd}^{2+}] + 0.4346$  with a correlation coefficient of 0.9972 and  $I_p(\mu\text{A}) = 0.2496[\text{Pb}^{2+}] + 0.2878$  with a correlation coefficient of 0.9968 ( $N=5$ ), respectively. The detection limits (LODs) for Cd<sup>2+</sup> and Pb<sup>2+</sup> were calculated as 0.12 and 0.21 μg/L, respectively. The remarkable results, such as good selectivity, repeatability, and reproducibility were obtained with the

modified electrode. Application of the sensors to milk samples produced recovery values in the range 95 to 102 %.

**Keywords** Differential pulse anodic stripping voltammetry · Heavy metal analysis · 3,8-diaminobenzo[*c*]cinnoline · Graphene oxide · Modified electrode

## Introduction

Benzo[*c*]cinnoline (BCC) and its derivatives are important compounds for dyes, photoconductors, polymers, and catalyst materials [1]. Some BCC derivatives are known for having mutagenic and herbicidal properties [2, 3]. BCC and its derivatives were electrografted on glassy carbon [4, 5], gold [6], and platinum electrode [7]. The structures of 3,8-diaminobenzo[*c*]cinnoline (3,8-DABCC) and its graphene composite at the surface are given in Scheme 1.

Graphene is a two-dimensional structure that the carbon atoms possess sp<sup>2</sup> hybridization [8]. It is designed as a building block for all other dimensions. Nanostructure, thermal variation, and remarkable mechanical and electrical properties of graphene have drawn attention continuously in material science [9]. Graphene derivatives are used in many fields such as bioelectronics, sensors, fuel cell, catalyst, etc. [10]. Because, it has the perfect surface area and conducting and low cost [11]. Graphene oxide (GO) is obtained by opening a single layer of graphite. The GO was used widely as electrode material on bare electrodes. In an article, Pd nanoparticle attached p-aminothiophenol (ATP) bridged graphene oxide was synthesized [12] with self assemble monolayer (SAM) and chemical methods. This electrode material was converted as reduced GO-ATP-Pd with an electrochemical method. The modified surface was used as material of biochemical sensor for determination of H<sub>2</sub>O<sub>2</sub>. In the literature, GO supported

A Festschrift in honor of Prof. Solak's 66th birthday and his recent retirement.

✉ Ali Osman Solak  
aliosman.solak@gmail.com

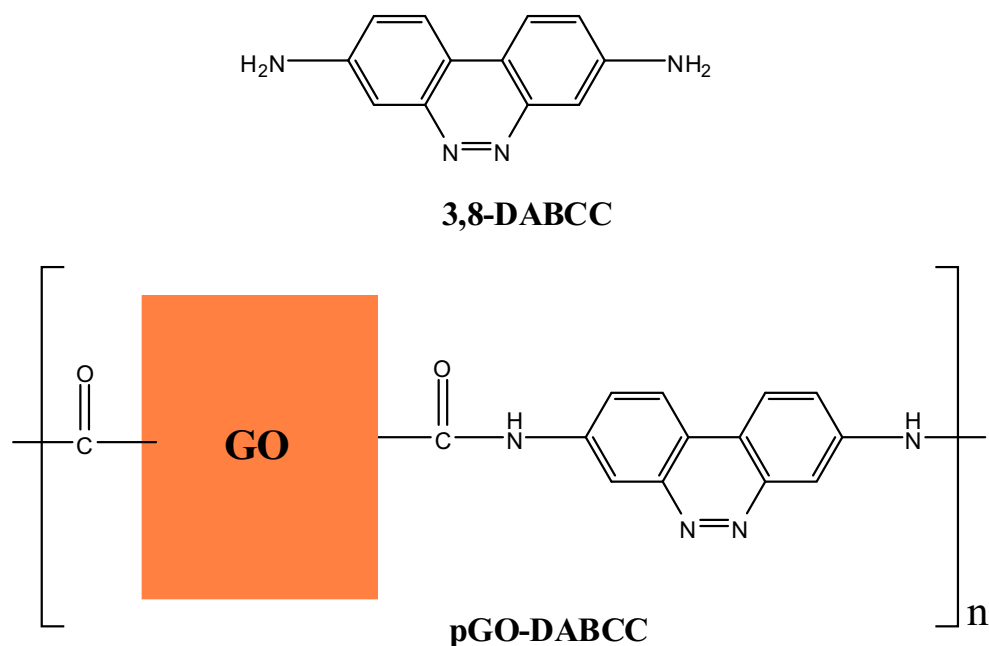
✉ Zafer Üstündağ  
zustundag@gmail.com

<sup>1</sup> Faculty of Arts and Science, Department of Chemistry, Dumlupınar University, 43100 Kutahya, Turkey

<sup>2</sup> Faculty of Science, Department of Chemistry, Ankara University, 06100 Ankara, Turkey

<sup>3</sup> Faculty of Engineering, Chem Eng Department, Kyrgyz-Turkish Manas University, Bishkek, Kyrgyzstan

**Scheme 1** Molecular structure of 3,8-DABCC and the proposed surface linkage in pGO-DABCC



platinum nanoclusters for methanol fuel cell application were prepared [13]. In addition, GO's polymers were used as electrode materials [14]. The mixtures of GO and aryl diamine compounds were polymerized together.

In this study, 3,8-DABCC was polymerized with polycarboxylate-included GO via amidization reaction. The

material was denoted as pGO-DABCC. It was characterized by IR and XPS. The material was covered on glassy carbon surface, and the surface was identified by electrochemical impedance spectroscopy (EIS) and cyclic voltammetry (CV). The electrode was used for the determination of  $\text{Cd}^{2+}$  and  $\text{Pb}^{2+}$  in aqueous media. The method was evaluated by

**Fig. 1** Cyclic voltammograms of 2-mM potassium ferrocyanide/ferricyanide system in 0.1-M KCl on **a** GC, GO and GC/pGO-DABCC (scan rate 200 mV/s) and **b** stability test of count of use of the GC/pGO-DABCC and GC/pGO-DABCC when it is kept in open atmosphere for 1 week, **c** Nyquist plots of 2-mM potassium ferrocyanide/ferricyanide system in 0.1-M KCl versus  $\text{Ag}/\text{AgCl}_{(\text{sat})}$

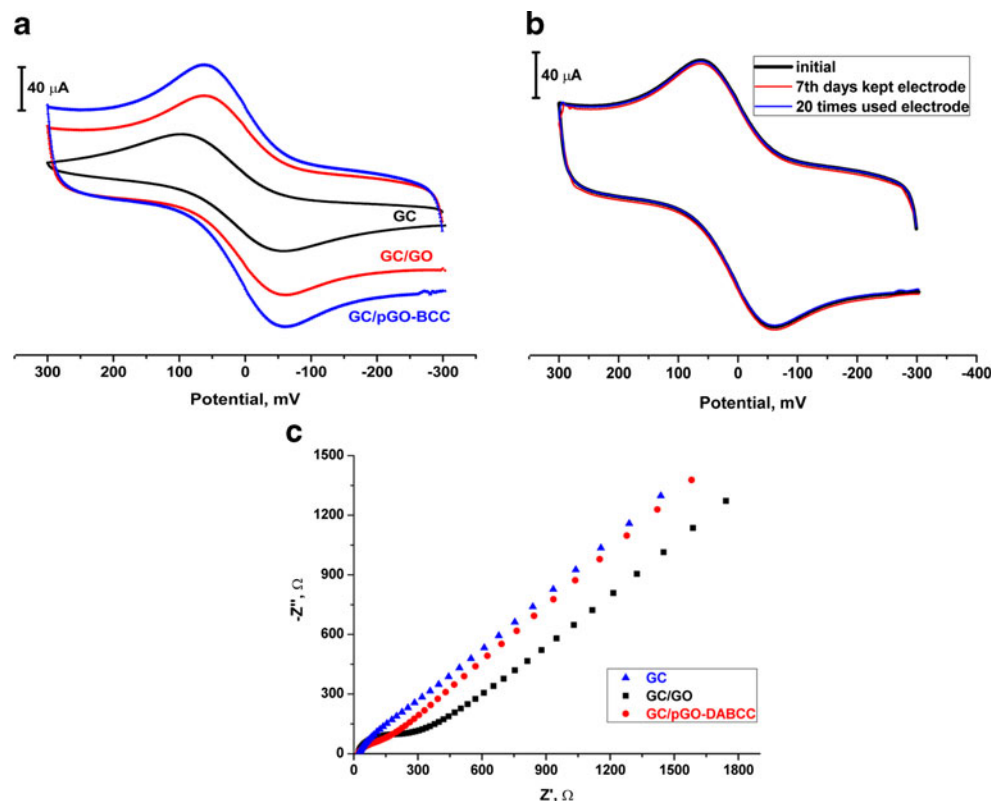
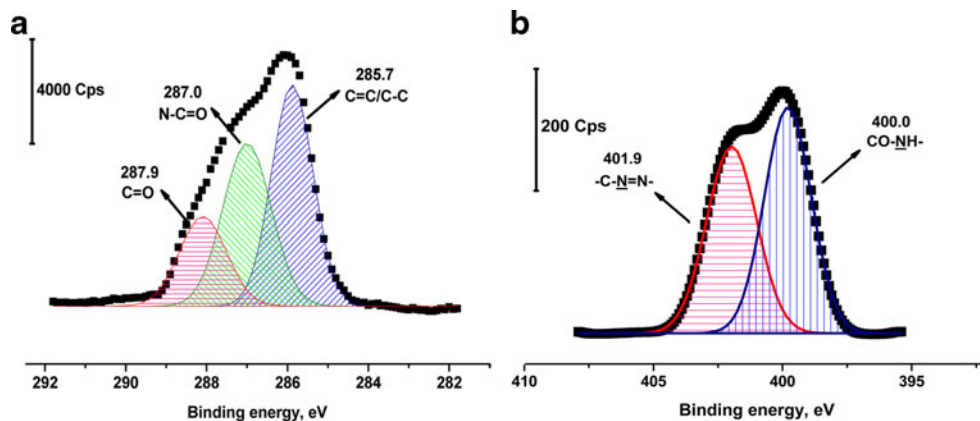


**Fig. 2** XPS core spectra of  $C_{1s}$  (a) and  $N_{1s}$  (b) of pGO-DABCC



application with the simultaneous determination of  $Cd^{2+}$  and  $Pb^{2+}$  ions in milk samples ( $n=6$ ) using the standard addition method.

## Materials and Methods

### Chemicals and Apparatus

All chemicals were purchased from Merck, Fluka, Sigma-Aldrich Riedel chemical company. 3,8-DABCC was synthesized by our research laboratory. MF-2012 glassy carbon (GC) working electrode was purchased from Bioanalytical Systems Company (USA). Bare GC electrodes were cleaned and polished on Buehler microfiber cloth (Lake Bluff, IL, USA) with 100 and 50 nM of the suspension of aluminum oxide (Baikowski, USA). Cleaned GC electrodes were sonicated with an ultrasonic bath cleaner (SK1200H, China) for approximately 6 min in ultrapure water (UPW, 18.2 M $\Omega$  cm, Human Power 1+, S. Korea) and mixture of 1:1 (v/v) isopropyl alcohol (IPA)/acetonitrile (MeCN) solutions. Voltammetric and impedimetric measurements were carried out under a high purified Ar (99.999 %) atmosphere by Ivium CompactStat, (US) electroanalyzer at room temperature ( $25 \pm 1$  °C) with triple electrode system. The reference and auxiliary electrodes were Ag/AgCl/KCl<sub>(sat)</sub> and platinum wire, respectively.

### Preparation of GO, pGO-DABCC, and GC/pGO-DABCC

3,8-DABCC was synthesized from 2,2'-dinitrobiphenyl, as described elsewhere [1]. It was prepared from the reduction of 2,2'-dinitrobiphenyl with hydrazine hydrate (100 %) in the presence of Pd-C (10 % Pd) catalyst in alkaline ethanol under reflux.

GO was synthesized with the method of electrochemical exfoliation of graphite as described elsewhere [15]. Platinum foil and pristine graphite were used as cathode and anode,

respectively, in a mixture of 2.4 g  $H_2SO_4$  and 11 mL of 30 % KOH in 100-mL UPW. The electrooxidation was carried out under the constant DC (Yıldırım Electronics, Turkey) potential of +20 V. Exfoliated product was sonicated with a Hermle (Z36HK, Germany) ultracentrifuge system under 12,000 rpm for 8 min and then washed with UPW. The GO was dried at 80 °C under vacuum for 8 h.

GO (0.2 g) was activated with 10-mM 1-ethyl-3-[3-dimethylaminopropyl]carbodiimide (EDC) [16] in 25 mL PBS (pH=7) and stirred via magnetic stirring for 6 h. The activated GO was participated with the centrifuge and then washed with UPW. It was added in 1 mM 3,8-DABCC included PBS (pH=7) solution and then stirred for 6 h. The amidized polymer bulk was sonicated and washed three times. It was dried at 100 °C for 2 h. One hundred milligrams of pGO-DABCC was diluted with 10 mL MeCN as suspension. The suspension was used for modified film on GC. The polished bare electrode (GC) was modified with 5, 10, 15, 20, and 25  $\mu$ L of sonicated 100-mg pGO-DABCC in 10-mL MeCN suspension by microsyringe, and then dried under an infrared lamp for 6 min [17]. The modified electrode

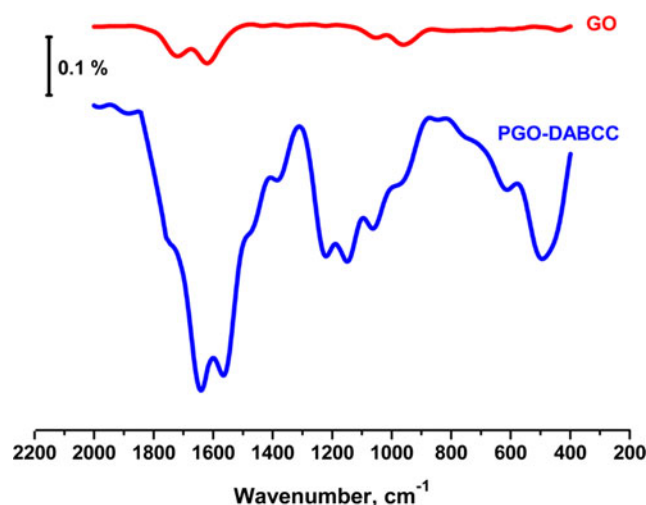


**Fig. 3** IR spectra of GO and pGO-DABCC

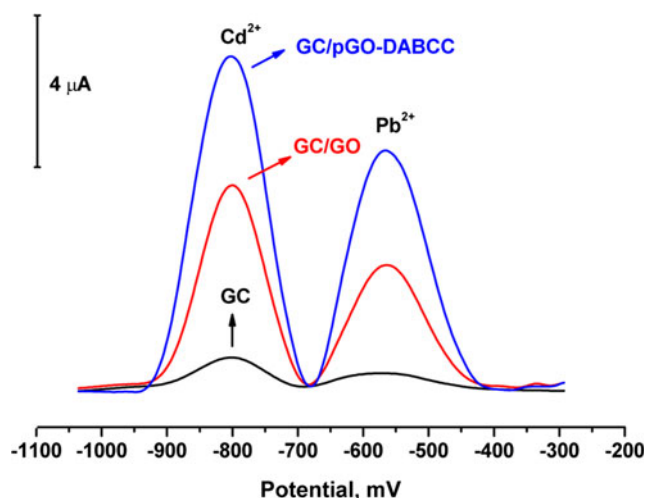


**Fig. 4** DPASV curves of 25  $\mu\text{M}$   $\text{Cd}^{2+}$  and  $\text{Pb}^{2+}$  on GG, GC/GO, and GC/pGO-DABCC in 0.1 M NaAc/HAc (incubation time 20 min, deposition potential  $-1.2$  V, amplitude 25 mV, and increment potential 2 mV)

was denoted as GC/GO-IPA. The polymer film covered GC was denoted as GC/pGO-DABCC.

### Characterization of pGO-DABCC and GC/pGO-DABCC

pGO-DABCC was characterized by infrared (IR) spectroscopy and X-ray photoelectron spectroscopy (XPS). Infrared spectroscopy measurement was performed by a Bruker (Tensor-27, Germany) Infrared spectrophotometer with a germanium crystal-included attenuated total reflectance system (GATR, Harrick Scientific, USA). A PHI 5000-Versa Probe ( $\Phi$  ULVAC-PHI, Inc., Japan/USA) with monochrome Al  $K\alpha$  radiation (1486.6 eV) as an X-ray anode and operated with 50 W at  $10^{-7}$  Pa was employed for the XPS measurements.

In addition, pGO-DABCC and GO films on GC were characterized by cyclic voltammetry (CV) and electrochemical impedance spectroscopy (EIS). Fifteen microliters of 100-mg pGO-DABCC in 10-mL MeCN solution and 15  $\mu\text{L}$  of 100-mg GO in 10-mL MeCN solution were dropped on bare GC surface. The modified surface was dried under IR lamp for 6 min.

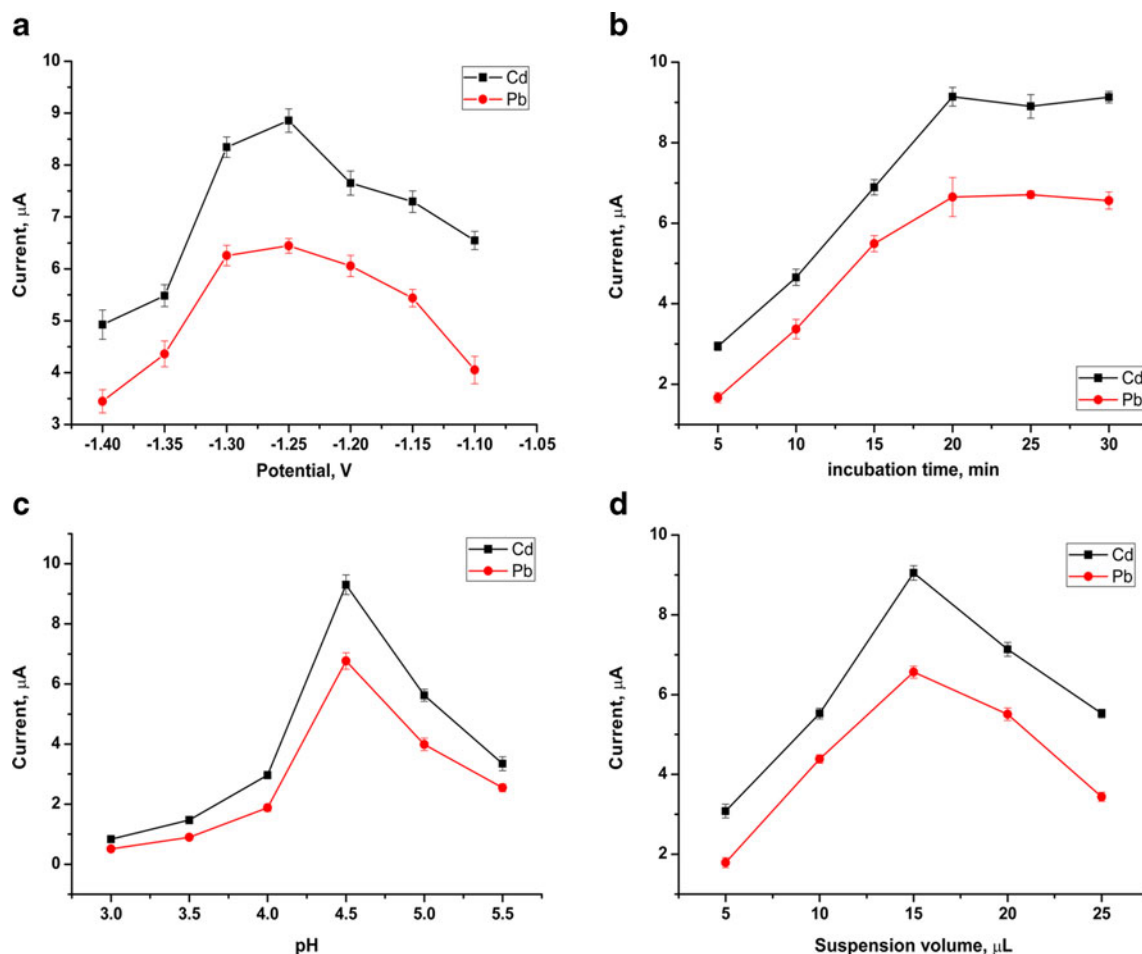
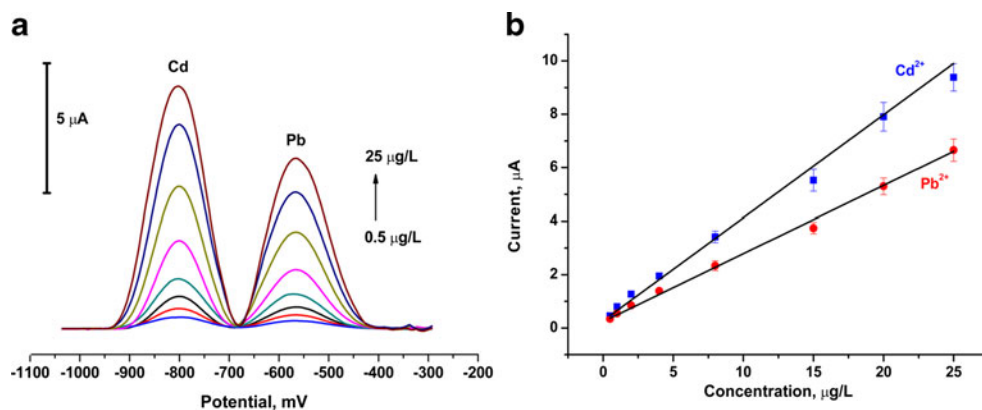


**Fig. 5** DPASV current optimum condition curves. The effect of deposition potential (a), incubation time (b), pH (c), and volume of suspension under other optimum conditions in 0.1-M NaAc/HAc at room temperature

**Fig. 6** DPASV curves (a) and their calibration curves (b) of  $\text{Cd}^{2+}$  and  $\text{Pb}^{2+}$  ranging from 0.5 to 20- $\mu\text{M}$  on GC/pGO-DABCC in 0.1-M NaAc–HAc buffer solution under optimum parameters



### Optimization of Measurement Conditions

The optimum parameters for analysis of heavy metals at pGO-DABCC modified GC were determined by DPASV. The conditions of measurement of  $\text{Cd}^{2+}$  and  $\text{Pb}^{2+}$  analysis on GC/pGO-DABCC at room temperature ( $25 \pm 1$  °C) were determined as few parameters such as constant potential, incubation time, pH, and volume of suspension on the electrode. The constant potential, incubation time, pH, and volume of suspension were studied in the range from  $-1.1$  to  $-1.40$  V, 5 to 30 min, 3 to 5.5, and 5 to 25  $\mu\text{L}$ , respectively, in 0.1 M sodium acetate/acetic acid buffer solution (NaAc/HAc).

### Determination of Simultaneous $\text{Cd}^{2+}$ and $\text{Pb}^{2+}$ in Aqueous Media with DPASV

Immersing of the GC/GO-DABCC electrode into the measuring solution containing  $\text{Cd}^{2+}$  and  $\text{Pb}^{2+}$  ions led to the accumulation of the ions on the electrode surface via complexation interaction under optimum conditions. The surface was taken off and washed with UPW. Before application the DPASV, metal ions on the modified electrode were reduced to metallic forms at  $-1.25$  V under the constant potential for 20 s in a measuring 0.1-M NaAc/HAc blank solution.

### Sample Treatment

Retail packaged milk samples were gathered from a local market in Turkey.  $\text{H}_2\text{O}_2$  (50  $\mu\text{L}$ ) (30 wt%) was added into 20-g milk sample under sonication in ultrasonic bath. The

solution was sonicated for 20 min. HCl (2.5 mL) (37 wt%) and 2.5-mL acetic acid (50 wt%) was added into the mixed solution, and then the last solution was sonicated for 10 min. The mixture was centrifuged with a Hermle Z36 HK centrifuge system under 10,000 rpm for 20 min. The supernatant was collected and filtered via a micropore membrane (Millex-FG, Ireland) with pore size of 200 nm. The filtrate was adjusted to pH 4.5 by NaAc/HAc buffer solution. The measurements of the samples were repeated six times ( $n=6$ ).

## Results and Discussion

### Electrode Modification and Characterization

Electrochemical characterization of modified surface was performed with CV and EIS techniques. Electrochemical behavior of the 2-mM potassium ferrocyanide/ferricyanide,  $\text{K}_3\text{Fe}(\text{CN})_6/\text{K}_4\text{Fe}(\text{CN})_6$ , in 0.1-M KCl solution was carried out with CV. The CVs are given in Fig. 1a. In the voltammograms, values of peak current of the redox couple probe on GC, GC/GO, and GC/pGO-DABCC are calculated as  $42.3 \pm 1.7$ ,  $53.0 \pm 3.4$ , and  $71.8 \pm 2.1$   $\mu\text{A}$ , respectively.

The stability of the pGO-DABCC film at the GC electrode was tested by ferrocene redox probe CV voltammograms in which the modified electrode was kept in an open atmosphere. Count of use of the surface was checked with the redox probe (Fig. 2b). It was observed that the surface was stable; within, it could be used 20 times. The figure shows the voltammogram of the redox probe in 0.1-M TBATFB in MeCN for the

**Table 1** Calibration data for the determination of  $\text{Cd}^{2+}$  and  $\text{Pb}^{2+}$  by the method ( $N=5$ )

Metals	$\text{Cd}^{2+}$	$\text{Pb}^{2+}$
Regression equation	$I_p(\mu\text{A}) = 0.3606[\text{Cd}^{2+}] + 0.4346$	$I_p(\mu\text{A}) = 0.2496[\text{Pb}^{2+}] + 0.2878$
$R^2$	0.9972	0.9968
Lineer range ( $\mu\text{g/L}$ )	0.5–25	0.5–25
LOD <sup>a</sup> ( $\mu\text{g/L}$ )	0.12	0.21

<sup>a</sup> Based on a signal-to-noise ratio equal to 3 ( $S/N=3$ )

**Table 2** Comparison of electroanalytical performance of some modified electrodes for Cd<sup>2+</sup> and Pb<sup>2+</sup>

Electrode	Method	Linear range (μg L <sup>-1</sup> )		Detection limit (μg L <sup>-1</sup> )		Ref.
		Cd <sup>2+</sup>	Pb <sup>2+</sup>	Cd <sup>2+</sup>	Pb <sup>2+</sup>	
GCE/NA-Graphene/BiF	DPASV	1.5–30	0.5–50	0.02	0.02	[20]
MWCNTs/NA/Bi/SPE	DPASV	0.5–80	0.05–100	0.1	0.01	[21]
GCE/SbF	DPASV	11.5–72.4	16.8–62.6	3.4	5.0	[22]
Bi/Nafion/ERGO–TH–MES/GCE	SWASV	1–40	1–40	0.1	0.05	[23]
Bi/Au–GN–Cys/GCE	SWASV	0.50–40	0.50–40	0.10	0.05	[24]
Nafion/Bi/NMC/GCE	DPASV	2–100	0.5–100	1.5	0.05	[25]
MWCNTs–Nafion/GCE	DPASV	0.08–100	0.05–100	0.04	0.025	[26]
GC/pGO–DABCC	DPASV	0.5–25	0.5–25	0.12	0.21	This work

Abbreviation of the electrode materials were used as original name

GCE glassy carbon electrode, CILE carbon ionic liquid electrode, BiF bismuth film, NA Nafion, DPASV differential pulse anodic stripping voltammetry, SPE screen-printed electrode, nitrogen doped microporous carbon, MNCNTs multiwalled carbon nanotubes, ERGO electrochemically reduced graphene oxide, MES 2-mercaptoethanesulfonate, TH thionine

modified electrode when it was kept in an open atmosphere for 1 week.

Charge transfer resistance of the redox couple on GC, GC/GO, and GC/pGO–DABCC was investigated with EIS. The Nyquist plots of the redox couple on GC, GC/GO, and GC/pGO–DABCC are illustrated in Fig. 1c. EIS measurements were recorded between 100 kHz and 0.2 Hz at 10 mV wave amplitude and at an electrode potential of 0.02 V of ferrocyanide/ferricyanide redox couple on bare and modified electrodes. Each plot was fitted as “CPE with diffusion” (Warburg effected CPE) equivalent electrical circuit. Charge transfer resistances of the redox couple on GC, GC/GO, and GC/pGO–DABCC were calculated as 401.8 ± 39.4, 255 ± 4.97, and 131.0 ± 7.1 Ω, respectively. It is obvious from the charge transfer values that the electron transfer rate of redox probe was accelerated in the case of GC/pGO–DABCC.

Spectroscopic characterization of the modified surface was carried out by infrared and X-ray photoelectron spectroscopy. XPS measurements were carried out only for pGO–DABCC. The C<sub>1s</sub> core spectrum for pGO–DABCC is given in Fig. 2a. As can be seen from the figure, broad XPS bands appeared between 284–290 eV in the C<sub>1s</sub> high-resolution spectrum. When the C<sub>1s</sub> region is curve fitted, the peaks appeared as C–C/C=C component at 285.7 eV, N–C=O group at 287.0 eV and –COOH peak at 287.9 eV. In Fig. 2b, two different N<sub>1s</sub> peaks in the core spectrum for pGO–DABCC were observed at about 400.0 and 401.9 eV, due to the CO–NH– and –C–N=N– groups, respectively.

FT-IR spectra of GO and pGO–DABCC are also given in Fig. 3. The spectra of GO have C=C and C=O stretching bands at 1620 and 1730 cm<sup>-1</sup>, respectively [18, 19]. For the covalently bonded GO and DABCC, the vibration band at 1377 cm<sup>-1</sup> could be assigned to the N–C=O stretching mode, the bands of 613 and 757 cm<sup>-1</sup> to C–H out of plane bending,

and the vibration band of 1466 cm<sup>-1</sup> to C–N=N– ring deformation. The band at 1150 and 1225 cm<sup>-1</sup> are assigned to the stretching vibrations of C–O and C–N, respectively [1].

### Optimization Results of the Measurements

DPASVs for determination of Cd<sup>2+</sup> and Pb<sup>2+</sup> on GC, GC/GO, and GC/pGO–DABCC electrode surface are depicted in Fig. 4. It can easily be seen that the oxidation peak current of Cd and Pb on GC/pGO–DABCC was larger than the other electrode. The anodic stripping potentials of Cd and Pb on GC/pGO–DABCC were determined as –0.805 and –0.567 V, respectively.

Some optimization parameters such as the constant potential, incubation time, pH, and volume of suspension of the electrochemical response of the GC/pGO–DABCC was investigated. Figure 5a–d shows the effect of constant potential values, optimum incubation time, pH, and volume of suspension, respectively.

**Table 3** Interference effect of some ions

Interfering ions	Signal change (%)	
	Cd <sup>2+</sup>	Pb <sup>2+</sup>
Na <sup>+</sup>	+0.2	+0.1
K <sup>+</sup>	+0.2	+0.3
Ca <sup>2+</sup>	+0.6	+0.4
Mg <sup>2+</sup>	+0.5	+0.3
Mn <sup>2+</sup>	–1.8	–1.2
Fe <sup>2+</sup>	–2.2	–2.6
Co <sup>2+</sup>	–2.3	–3.2
Ni <sup>2+</sup>	–2.7	–2.3

**Table 4** Precision and accuracy results of the methods

Day <sup>a</sup>	Values	Ions	Added (Cd <sup>2+</sup> , Pb <sup>2+</sup> )	
			3 µg/L	7 µg/L
Intraday	Found Value	Cd <sup>2+</sup>	3.10±0.02	6.98±0.03
		Pb <sup>2+</sup>	3.05±0.01	7.04±0.04
	Accuracy (%)	Cd <sup>2+</sup>	3.33	-0.29
		Pb <sup>2+</sup>	1.67	0.57
	Precision (%)	Cd <sup>2+</sup>	0.65	0.43
		Pb <sup>2+</sup>	0.33	0.57
Interday	Found value	Cd <sup>2+</sup>	2.97±0.02	7.03±0.05
		Pb <sup>2+</sup>	3.00±0.04	6.98±0.03
	Accuracy (%)	Cd <sup>2+</sup>	1.00	0.43
		Pb <sup>2+</sup>	0.00	-0.29
	Precision (%)	Cd <sup>2+</sup>	0.67	0.71
		Pb <sup>2+</sup>	1.33	0.43

<sup>a</sup> Five independent series on the same day for intraday precision and five consecutive days for interday precision from five measurements of every series

The stripping peak currents of both ions increased by increasing constant or deposition potential in the range -1.4 to -1.25 V and decreased at higher potentials at room temperature, 15 µL of suspension volume, incubation time of 20 min, and pH under 4.5. Before recording the stripping currents, metal ions complexed on the GC/pGO-DABCC electrode surface were reduced at -1.25 V for 20 s in a measuring blank solution. The optimum potential was chosen as -1.25 V (Fig. 5a). Similarly, incubation time (Fig. 5b), pH (Fig. 5c), and volume of suspension (Fig. 5d) were detected as 20 min,

4.5, and 15 µL, respectively, at -1.25 V and under other optimum conditions.

### Calibration Studies of Cd<sup>2+</sup> and Pb<sup>2+</sup> on the GC/GO

The calibration curves was obtained with DPASV measurement of various concentrations of Cd<sup>2+</sup> and Pb<sup>2+</sup> ranging from 0.5 to 20 µM in 0.1-M NaAc/HAc in 0.1-M NaAc/HAc at room temperature under the optimized conditions (15 µL of suspension volume, incubation time of 20 min, and pH under 4.5).

DPASV voltammograms of Cd<sup>2+</sup> and Pb<sup>2+</sup> ranging from 0.5 to 20 µM on GC/pGO-DABCC in 0.1-M NaAc-HAc buffer solution and their calibration curves are given in Fig. 6. The calibration data for the simultaneous determination of metals by developed method is illustrated in Table 1. Comparison of the modified electrode and other electrodes for determination of Cd<sup>2+</sup> and Pb<sup>2+</sup> is given in Table 2.

The detection limits (LODs) for Cd<sup>2+</sup> and Pb<sup>2+</sup> were determined as 0.12 and 0.21 µg/L, respectively. Under the optimum conditions, a linear relationship existed between the currents and the concentrations of the ions in the range between 0.50 and 25 µg/L. LOD results in the range of the developed method especially for Cd<sup>2+</sup> are not bad according to many studies [20–29].

### Interference Effect of Some Metals

Interference effect of the methods was performed with possible interferences of some ions such as Na<sup>+</sup>, K<sup>+</sup>, Ca<sup>2+</sup>, Mg<sup>2+</sup>, Mn<sup>2+</sup>, Fe<sup>2+</sup>, Co<sup>2+</sup>, and Ni<sup>2+</sup>. Cd<sup>2+</sup> and Pb<sup>2+</sup> (25 µg/L) with

**Table 5** Simultaneous determination of Cd<sup>2+</sup> and Pb<sup>2+</sup> in milk samples and their recovery values (n = 6)

Sample	Added, µg/kg <sup>a</sup>		DPASV, µg/kg		ICP-OES, µg/kg		Recovery (%)	
	Cd <sup>2+</sup>	Pb <sup>2+</sup>	Cd <sup>2+</sup>	Pb <sup>2+</sup>	Cd <sup>2+</sup>	Pb <sup>2+</sup>	Cd <sup>2+</sup>	Pb <sup>2+</sup>
S-1	–	–	1.27±0.11	3.41±0.33	–	3.35±0.32	–	–
	5	5	6.32±0.72	8.63±0.78	6.40±0.77	8.47±0.62	99.2	97.4
	10	10	11.19±0.96	13.36±0.85	11.27±0.82	13.51±0.93	100.7	100.4
S-2	–	–	1.13±0.17	5.05±0.45	–	4.92±0.51	–	–
	5	5	6.19±0.88	10.07±0.51	6.22±0.71	9.63±0.66	99.0	99.8
	10	10	11.27±0.73	14.91±1.87	11.41±0.80	15.11±1.93	98.7	100.9
S-3	–	–	2.53±0.28	2.04±0.20	–	2.11±0.25	–	–
	5	5	7.44±0.75	7.14±0.79	7.38±0.59	7.01±0.84	101.2	98.6
	10	10	13.08±1.06	11.97±0.92	12.95±0.92	12.29±1.20	95.6	100.6
S-4	–	–	1.86±0.21	7.61±0.58	–	7.49±0.67	–	–
	5	5	6.75±0.55	12.49±1.24	6.71±0.41	12.58±0.93	101.6	101.0
	10	10	12.06±1.22	17.92±1.41	12.21±0.84	17.71±1.68	98.3	98.3
S-5	–	–	1.95±0.26	2.27±0.25	–	2.33±0.32	–	–
	5	5	7.04±0.67	7.45±0.33	7.13±0.58	7.38±0.73	98.7	97.5
	10	10	11.80±0.93	12.15±0.54	11.94±0.87	12.42±1.41	101.3	101.0

<sup>a</sup> µg/L was converted to µg/kg

other metal ions in a 300-fold mass ratio of interference to analyte were investigated at the GC/pGO-DABCC surface. The analysis results are given in Table 3. The data shows that the signal deviation of 25  $\mu\text{g/L}$   $\text{Cd}^{2+}$  and  $\text{Pb}^{2+}$  do not rise larger than 4 %.

### Precision and Accuracy of the Methods

Two different concentrations of  $\text{Cd}^{2+}$  and  $\text{Pb}^{2+}$  in the linear range were analyzed in five independent series on the intraday and interday. The results as percent data are listed in Table 4. The RSD (precision) % values varied from 0.33 to 1.33 for intraday and interday precision of  $\text{Cd}^{2+}$  and  $\text{Pb}^{2+}$ . Accuracy of the investigated method was calculated as the percent relative error. Both of the results obtained for intraday and interday accuracy were <4.00 %.

### Analysis of Milk Samples

To evaluate, the accuracy of developed sensor was employed to determine  $\text{Cd}^{2+}$  and  $\text{Pb}^{2+}$  in milk sample extracts. Recoveries of  $\text{Cd}^{2+}$  and  $\text{Pb}^{2+}$  response of the method were up to 95 %. The analysis results were checked by ICP-OES. The recovery values of  $\text{Cd}^{2+}$  and  $\text{Pb}^{2+}$  in real samples ( $n=6$ ) are given in Table 5. The values of analysis were given as  $\mu\text{g/kg}$  with  $[C_{\text{sample}} (\mu\text{g/kg})] = [C_{\text{extracted solution}} (\mu\text{g/L})] \times 40 \text{ mL} / 40 \text{ g}$  [30]. The value of  $[C_{\text{extracted solution}}]$  was calculated with the method proposed in this study.

### Conclusion

Diamine-included 3,8-DABCC was polymerized with GO. The material was characterized with IR and XPS. It was attached on GC. The modified electrode was characterized by using CV and EIS techniques. A novel sensitive method with the modified electrode was investigated for simultaneous determination of  $\text{Cd}^{2+}$  and  $\text{Pb}^{2+}$  in aqueous media. The calibration equations were acquired as  $I_p(\mu\text{A}) = 0.3606[\text{Cd}^{2+}] + 0.4346$  with a high correlation coefficient of 0.9972 for  $\text{Cd}^{2+}$  and  $I_p(\mu\text{A}) = 0.2496[\text{Pb}^{2+}] + 0.2878$  with a high correlation coefficient of 0.9968 for  $\text{Pb}^{2+}$  ( $N=5$ ). The LODs for  $\text{Cd}^{2+}$  and  $\text{Pb}^{2+}$  were calculated as 0.12 and 0.21  $\mu\text{g/L}$ , respectively. The method was evaluated by application with the simultaneous determination of  $\text{Cd}^{2+}$  and  $\text{Pb}^{2+}$  in milk samples. The features of nanosensor were investigated. It has good selectivity and has low LOD. Repeatability and reproducibility of the method is good enough. The recoveries of the  $\text{Cd}^{2+}$  and  $\text{Pb}^{2+}$  response of the method were up to 95 %.

### References

1. A.A. İ-Turan, E. Kılıç, Z. Üstündağ, H. Ekşi, A.O. Solak, B. Zorer, *J. Solid State Electron.* **16**, 235–245 (2012)
2. J.A. Leary, A.L. Lafleur, H.L. Liber, K. Biemann, *Anal. Chem.* **55**, 758–761 (1983)
3. I.D. Entwistle, T. Gilkerson, J.W. Barton, UK Patent. GB2059263 (1981)
4. A.A. İ-Turan, Z. Üstündağ, A.O. Solak, E. Kılıç, A. Avseven, *Electroanalysis* **20**, 1665–1670 (2008)
5. A.A. İ-Turan, Z. Üstündağ, E. Kılıç, R. Güzel, Ö. Uçkan, A.O. Solak, *Instrum. Sci. Technol.* **39**, 149–160 (2011)
6. Z. Üstündağ, A.A. İ-Turan, A.O. Solak, E. Kılıç, A. Avseven, *Instrum. Sci. Technol.* **37**, 284–302 (2009)
7. A.A. İ-Turan, Z. Üstündağ, A.O. Solak, E. Kılıç, A. Avseven, *Thin Solid Films* **517**, 2871–1877 (2009)
8. K. Zhang, L.L. Zhang, X.S. Zhao, J. Wu, *Chem. Mater.* **22**, 1392–1401 (2010)
9. T.J. Davies, M.E. Hyde, R.G. Compton, *Angew. Chem, Int. Edit* **44**, 5121–5126 (2005)
10. L. Cunci, C.V. Rao, C. Velez, Y. Ishikawa, C.R. Cabrera, *Electrocatalysis* **4**, 61–69 (2013)
11. K. Kakaei, *Carbon* **51**, 195–201 (2013)
12. J.-M. You, D. Kim, S.K. Kim, M.-S. Kim, H.S. Han, S. Jeon, *Sensor. Actuat. B-Chem.* **178**, 450–457 (2013)
13. K. Ji, G. Chang, M. Oyama, X. Shang, X. Liu, Y. He, *Electrochim. Acta* **85**, 84–89 (2012)
14. H.S. Han, J.-M. You, H. Jeong, S. Jeon, *Appl. Surf. Sci.* **284**, 438–445 (2013)
15. A. Erkal, M.S. Erdoğan, İ. Aşık, H. Ekşi, S. Jeon, A.O. Solak, Z. Üstündağ, *J. Electrochem. Soc.* **161**, H696–H704 (2014)
16. K. Sablok, V. Bhalla, P. Sharma, R. Kaushal, S. Chaudhary, C.R. Suri, *J. Hazard. Mater.* **248–249**, 322–328 (2013)
17. A. Erkal, İ. Üstündağ, S. Yavuz, Z. Üstündağ, *J. Electrochem. Soc.* **162**, H213–H219 (2015)
18. H.S. Han, H.K. Lee, J.-M. You, H. Jeong, S. Jeon, *Sensor. Actuat. B-Chem.* **190**, 886–895 (2014)
19. F. Li, L. Guosong, J. Baohua, Y. Aimin, *Electrocatalysis* **6**, 72–76 (2015)
20. X. Guo, Y. Yun, V.N. Shanov, H.B. Halsall, W.R. Heineman, *Electroanalysis* **23**, 1252–1259 (2011)
21. L. Fu, X. Li, J. Yu, J. Ye, *Electroanalysis* **25**, 567–572 (2013)
22. V. Sosa, C. Barceló, N. Serrano, C. Ariño, J.M. D.-Cruz, M. Esteban, *Anal. Chim. Acta* **855**, 34–40 (2015)
23. Z. Li, L. Chen, F. He, L. Bu, X. Qin, Q. Xie, S. Yao, X. Tu, X. Luo, S. Luo, *Talanta* **122**, 285–292 (2014)
24. L. Zhu, L. Xu, B. Huang, N. Jia, L. Tan, S. Yao, *Electrochim. Acta* **115**, 471–477 (2014)
25. L. Xiao, H. Xu, S. Zhou, T. Song, H. Wang, S. Li, W. Gan, Q. Yuan, *Electrochim. Acta* **143**, 143–151 (2014)
26. H. Xu, L.P. Zeng, S.J. Xing, Y.Z. Xian, G.Y. Shi, *Electroanalysis* **20**, 2655–2662 (2008)
27. K. Keawkim, S. Chuanwatanakul, O. Chailapakul, S. Motomizu, *Food Control* **31**, 14–21 (2013)
28. P.K.Q. Nguyen, S.K. Lunsford, *J. Electroanal. Chem.* **711**, 45–52 (2013)
29. G.H. Hwang, W.K. Han, J.S. Park, S.G. Kang, *Talanta* **76**, 301–308 (2008)
30. J. Ping, Y. Wang, J. Wu, Y. Ying, *Food Chem.* **151**, 65–71 (2014)